# Post-seismic settlement mitigation for a building in Richmond, B.C.

Mustapha Zergoun and Ivan Rivera Cruz
*Thurber Engineering Ltd., Vancouver, B.C., Canada*

ABSTRACT
This paper describes the ground improvement scheme implemented to mitigate post-seismic settlement of a building in Richmond, British Columbia. The site topography is flat and below the expected regional flood level. The site is in a seismically active zone with shallow groundwater level. The subsoil stratigraphy includes loose sand deposits which are potentially liquefiable under a strong seismique event. The building foundations consisted of spread footings and the soil liquefaction mitigation included vibro-replacement soil densification. Due to site and economic restraints, the mitigation scheme did not extend to the full depth of the potentially liquefiable soils and its lateral extent was limited to the building perimeter. Therefore, vertical seismic drains were installed along the building perimeter to mitigate potential adverse effects on the building due to excess pore pressure generated during an earthquake. The paper outlines how the soil densification target criteria were established and points out the limitations of the vibro-replacement method. The paper describes the methods available to assess the building post-seismic settlement.

RÉSUMÉ
Cet article décrit l'atténuation du tassement post-sismique d'un bâtiment à Richmond, Colombie-Britannique. La topographie du site est plate et en-dessous du niveau prévu de crue régionale. Le site est dans une zone d'activité sismique et la nappe d'eau est proche de la surface. La stratigraphie des sols inclut un dépôt de sable lâche qui est potentiellement liquéfiable en cas d'un fort séisme. Les fondations du bâtiment consistaient de semelles et l'amélioration du sol contre la liquéfaction comprenait la densification des sols par vibro-remplacement. En raison des contraintes dues au site et des conditions économiques, l'amélioration ne s'étendait pas à la profondeur totale des sols liquéfiables et son étendue latérale était limitée au périmètre du bâtiment. Par conséquent, des drains verticaux ont été installés le long du périmètre du bâtiment pour atténuer la liquéfaction des sols sous le bâtiment. Cet article montre comment le critère de densification des sols a été établi et montre les limites de la méthode de vibro-remplacement. Cet article décrit les méthodes disponibles pour estimer le tassement post-sismique du bâtiment.

## 1 INTRODUCTION

Significant advances have been made in the liquefaction assessment of loose sand and silt deposits under seismic conditions (Boulanger and Idriss, 2016). Empirical procedures are available to estimate post-liquefaction, free-field, one-dimensional consolidation settlement and horizontal ground deformations (Ishihara and Yoshimine, 1992, Zhang et al, 2002 and 2004, Boulanger and Idriss, 2014). However, the estimation of post-seismic shear-induced and ejecta-induced settlement of buildings (Bray and Macedo, 2017) is rarely undertaken in geotechnical engineering practice. This would be particularly useful for sites that underwent soil liquefaction remediation but lacked the benefit of direct observations or historic records of performance of building after a real earthquake event.

After remediation to mitigate potential soil liquefaction, the estimation of post-seismic settlement of buildings remains to be documented in geotechnical engineering practice. This paper describes the site preparation that was undertaken to mitigate post-seismic settlement for a building located in Richmond, British Columbia. The paper also outlines the methods available to assess the building post-seismic settlement.

The proposed building site is in the Fraser River Delta, at 8251 St Albans Road, south of Blundell Road, Richmond, British Columbia. The new building has a simple configuration and covers a square area of about 1470 m$^2$ as shown in Figure 1. The proposed building is bounded by an existing one-story wood frame church hall building and a surface parking area to the north and west, respectively, and another existing small office type building to the south. Municipal underground services exist along the east side, between the existing buildings and the adjacent roadway. The existing buildings and underground services formed constraints for the proposed development and required site preparation.


Figure 1 Proposed building plan

The proposed building consisted of a one-storey concrete, steel and timber structure with wide spans to accommodate a larger new church hall. The top of the sloped floor slab ranged from El. 1.6 to El. 1.8 m, which

was about 0.3 to 0.5 m above the centreline elevation of the adjacent St Albans Road.

## 2 SITE AND SUBSURFACE CONDITIONS

The site topography was relatively flat, and the grade elevation ranged between 1.0 and 1.2 m with reference to a geodetic datum. Although a series of protective dykes surround the deltaic City of Richmond, the site is considered subject to flood risk from the nearby Fraser River if the dyke structure is breached by a severe flood event exceeding the 1 in 200 years rate of occurrence assumed for design or under a strong seismic event.

Figure 2 shows the location of three test holes that were completed during our preliminary site investigation in 2016. The test holes included one Cone Penetration Test (CPT96-01) with pore water pressure measurement and two auger holes with soil sampling at regular depths.


Figure 2 Test hole location plan in 2016 site investigation
A = CPT96-01 B = AH96-01 C = AH96-02

The test holes indicated that the soil profile can be expected to be relatively uniform within the site. Table 1 provides a summary of the subsoil stratigraphy expected under the proposed building area. It consisted of a thin layer of compact to dense fill overlying soft and compressible silty clay to clayey silt, overlying compact to dense silty sand and sandy silt, overlying compact to dense interlayered sand and silty sand, overlying soft, compressible layered silt and clayey silt to the maximum depth of site investigation of 30 m.

Table 1 Generalized subsoil profile

| Deposit | Depth (m) | Soil description |
|---|---|---|
| Fill | 0 - 0.5 | Compact silt, sand and gravel |
| Silty clay to clayey silt | 0.5 - 3 | Soft, compressible layered silty clay to clayey silt, some organics |
| Silty sand, sandy silt | 3 - 5 | Compact to dense layered silty sand, sandy silt, fine sand |
| Sand to silty sand | 5 - 18 | Compact to dense fine sand, some silt |
| Silt to clayey silt | 18 - 30 (*) | Soft, compressible layered silt and clayey silt |

Figure 3 shows the shear wave velocity with depth measured by the Geological Survey of Canada in 1990 at test hole FD90-1 located near Richmond City Hall, which is located about 1.5 km northwest of the site. The shear wave velocity increased from 120 to 220 m/s in the top 50 m and then gradually increased to 600 m/s down to 300 m depth. The bedrock was not encountered at that depth.
Figure 3 Shear wave velocity versus depth used in SSRA

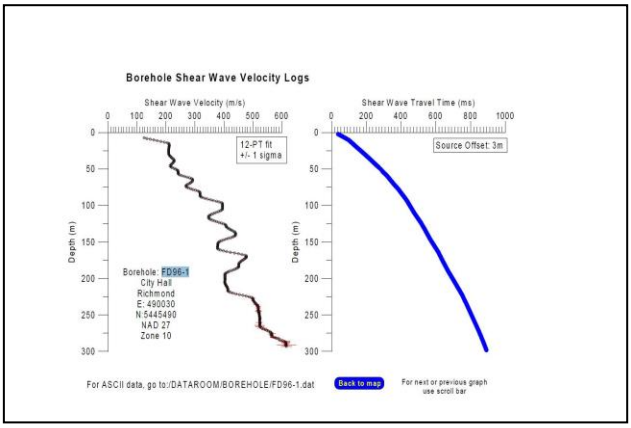


The natural water content measured in the laboratory on samples from the silty clay to clayey silt layer at a depth of 0.9 m to 1.2 m ranged from 34% to 70% with an average value of about 50%. The Atterberg limits measured in the laboratory on a sample from the silty sand to sandy silt at depth of 2.1 m were: liquid limit = 37%, plastic limit = 28%, and plasticity index = 9%. The natural water content measured in the laboratory on samples from the silty sand to sandy silt at a depth of 3.2 m to 4.0 m ranged from 28% to 31%. The fines content passing sieve No. 200 (0.075 mm) from a sample at 3.2 m was about 48%.

The above test results indicated that both soil units in the depth ranging from 0.5 to 5 m are considered cohesive and compressible under vertical effective stresses exceeding the existing overburden pressure.

Based on the interpretation of measured pore water pressure dissipation tests during CPT96-01, the groundwater level was estimated at about 1.0 m depth at the time of drilling. The groundwater level is expected to be influenced by tidal and seasonal fluctuations.

## 3 PROBABILISTIC SEISMIC HAZARD

The provisions for seismic design in the latest National Building Code of Canada (NBCC 2015) incorporated the 5$^{th}$ generation probabilistic seismic hazard model (SHM) developed by the Geological Survey of Canada (GSC). The GSC provided the deaggregation of seismic hazard values for Site Class C, with an exceedance rate of 2% in 50 years, of the pre-calculated grid point located closest to the project site for periods ranging from 0.05 to 10 seconds (Liam Finn et al. 2016).

The deaggregation identified the contribution to the total seismic hazard from three earthquake sources: a) Crustal; b) In-slab; and, c) Interface. The results were organized in bins. Each bin was 0.1 magnitude wide and 20 km long.

For convenience, the contributions from each bin were given per mil (1000). These can be divided by 10 to obtain the percent contribution.

The numbers listed in the deaggregation matrix corresponded to the total contributions of each bin versus two parameters: a) Hypocentral distance from the site to the earthquake source; and, b) Earthquake magnitude.

We used the deaggregation information provided by the GSC to weigh the relative contribution from each bin to the total hazard. These weighting factors were applied to the spectral acceleration obtained from the site-specific seismic ground response assessment (SSRA). We adopted a criterion based on hypocentral distance and magnitude to group the bins and distinguish between the three earthquake sources for the site.

The total contribution per source corresponded to the sum of the bin contributions. The sum of the contributions per source is 100%. We used linear interpolation to obtain the hazard contribution for intermediate periods. Table 2 summarizes the contribution factors applied to the results of our SSRA.

Table 2 Site-specific probabilistic seismic hazard

| Period (s) | Crustal Earthquakes | | In-slab Earthquakes | | Interface Earthquakes | |
|---|---|---|---|---|---|---|
| | Sum | Contribution (%) | Sum | Contribution (%) | Sum | Contribution (%) |
| 0.05 | 175 | 17.5 | 798 | 79.8 | 26 | 2.6 |
| 0.10 | 172 | 17.2 | 785 | 78.5 | 40 | 4.0 |
| 0.20 | 113 | 11.3 | 838 | 83.8 | 47 | 4.7 |
| 0.30 | 80 | 8.0 | 836 | 83.6 | 82 | 8.2 |
| 0.50 | 61 | 6.1 | 781 | 78.1 | 151 | 15.1 |
| 1.00 | 54 | 5.4 | 562 | 56.2 | 382 | 38.2 |
| 2.00 | 30 | 3.0 | 425 | 42.5 | 537 | 53.7 |
| 5.00 | 26 | 2.6 | 103 | 10.3 | 869 | 86.9 |
| 10.00 | 14 | 1.4 | 79 | 7.9 | 902 | 90.2 |

a) Hazard contribution based on interpretation of deaggregation of seismic hazard provided by the Geological Survey of Canada for Point No. 34072
b) Sum of hazard contributions are given per mil (1000)

## 4 SITE-SPECIFIC SEISMIC GROUND RESPONSE ASSESSMENT

The results of our 2016 site investigation as well as subsurface information available from nearby sites indicated the presence of soil deposits susceptible to liquefaction and soft to stiff silty clay deposits with thickness greater than 30 m. The soil stratigraphy at the project site met the requirements of Site Class F ("Other Soils") for seismic design as defined by NBCC 2015.

One dimensional site-specific seismic ground response assessment (SSRA) was carried out using the computer program SHAKE2000 to determine the spectral accelerations ($S_a$) at the ground surface for the site for periods ranging from 0.01 to 10 seconds. The program computed the seismic ground response of a soil column subjected to vertically propagating shear waves. These waves propagated from the underlying Site Class C dense layer (bedrock) to the ground surface to simulate earthquake induced shaking. The soil column was assumed to consist of several homogeneous visco-elastic layers of infinite horizontal extent and a half space as the bottom layer.

Each soil strata type was characterized by its thickness, unit mass, shear wave velocity ($V_s$), shear modulus degradation ($G/G_0$) and damping ratio ($\varphi$) curves. Non-linearity of the soil deposits was accounted for using an equivalent linear constitutive model which obtained values of shear stiffness and damping that were compatible with the effective shear strains in each layer through an iterative procedure.

The design $V_s$ profile was obtained from published data collected by the Geological Survey of Canada (GSC) near Richmond City Hall. See test hole FD90-1 on Figure 3. For analysis purposes, the base of the one-dimensional soil column was assumed at the bottom the Pleistocene deposits, which was estimated at 160 m depth with shear wave velocity values ranging from 736 to 760 m/s (Soil Class C).

The calculations were completed using available published shear modulus degradation ($G/G_0$) and damping ratio ($\varphi$) curves. For the Holocene deltaic deposits, the average $G/G_0$ and $\varphi$ curves by Seed & Idriss (1970) for sand and those by Vucetic and Dobry (1991) dependent on plasticity index (PI) were used for sand/silty sand and clayey silt layers, respectively. For the Pleistocene deposits and underlying Site Class C dense layer , the $G/G_0$ and $\varphi$ curves for gravel by Seed et al. (1986) and EPRI (1993) Rock 4 curves (121 to 250 feet) were used, respectively.

The 2007 Task Force Report on geotechnical design guidelines for buildings on liquefiable sites in Greater Vancouver in accordance with NBC 2005 provided recommendations for the selection of the plasticity index (PI) values for fine-grained sediments in the Fraser River Delta. Based on the thickness of marine fine-grained deposits used in our analyses and the guidelines in the 2007 Task Force Report, an average PI of 15 was selected for the clayey silt below 18 m depth.

The input earthquake ground motions comprised suites of ground motions for the design earthquake representative of crustal, in-slab and interface earthquake sources. Each suite contains ten pre-selected strong motion acceleration records. Each acceleration record was scaled linearly so that the peak ground acceleration and average response spectrum of each suite was not less than 1.10 times the deaggregated Site Class C target response spectrum for each earthquake source over the periods of interest.

Figure 4 shows the estimated response spectra for 5% damping at the ground surface for the 2,475-year return period. The response spectra from NBCC 2015 Site Class E, D and C are also shown for comparison purposes.

The spectral acceleration at zero period on the estimated site-specific response spectrum was considered as the PGA, equal to 0.2g. Both the PGA value and the Cyclic Stress Ratio (CSR) versus depth from each of the three earthquake sources were used for our soil liquefaction assessment. The spectral acceleration at one second period ($S_{a1}$) equal to 0.5g on the average response

was used for the estimation of post-seismique building settlement.

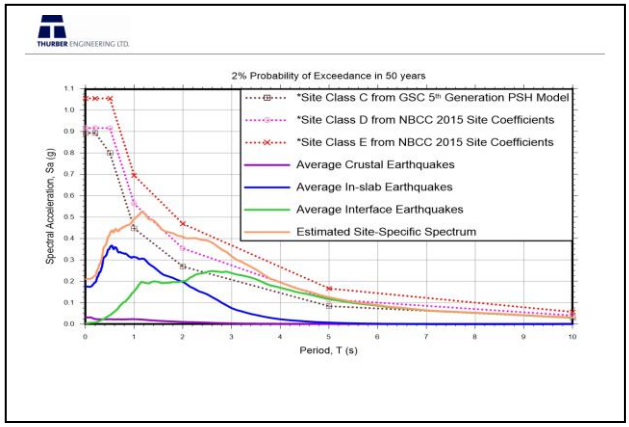


Figure 4 Response spectra at the ground surface for the 2,475-year return period seismic event with 5% damping

## 5 SOIL LIQUEFACTION ASSESSEMENT

The safety factor against the trigger of soil liquefaction ($FS_{LIQ}$) was calculated using the CPT-based simplified procedure proposed by Boulanger and Idriss (2014). The $FS_{LIQ}$ is the Resistance Cyclic Ratio (CRR) divided the Cyclic Stress Ratio (CSR). The commercial software program CLiq was used for this assessment.

In our soil liquefaction assessment, we used both the deterministic CSR calculated using PGA = 0.2g as well as the CSR versus depth derived from our SSRA for each of the three probabilistic earthquake sources. Soil liquefaction can be triggered when the $FS_{LIQ}$ is less than 1.0 i.e. CRR is less CSR.

Figure 5 shows that for CPT06-01, soil liquefaction can be triggered by a 2475-year earthquake in loose soil deposits below the groundwater level. The total thickness of potentially liquefiable soil ($H_L$) is estimated at 13.5 m for PGA = 0.2g, 10.8 m for crustal earthquakes, 14.0 m for in-slab earthquakes and 14.5 m for interface earthquakes.

Consequently, before soil densification, post-seismic settlement and horizontal ground deformations can occur within this site. The crustal earthquakes resulted in the lowest thickness of liquefiable soil while the interface earthquakes resulted in the largest thickness of liquefiable soils. The soil liquefaction thickness calculated using PGA = 0.2g was equal to the average of the four methods.

## 6 POST-LIQUEFACTION SOIL BEARING CAPACITY ASSESSMENT

The post-liquefaction soil bearing capacity factor of safety (*FS*) is calculated to be 0.78 using the Meyerhof and Hanna (1978) method with a residual strength of the liquefied soil layer of 12 kPa (based on Idriss and Boulanger 2008) and an average shear strength of the non-liquefied crust layer of 20 kPa (based on CPT16-01). As the post-liquefaction soil bearing capacity FS is less than 1.0, significant liquefaction-induced building settlement would likely occur.

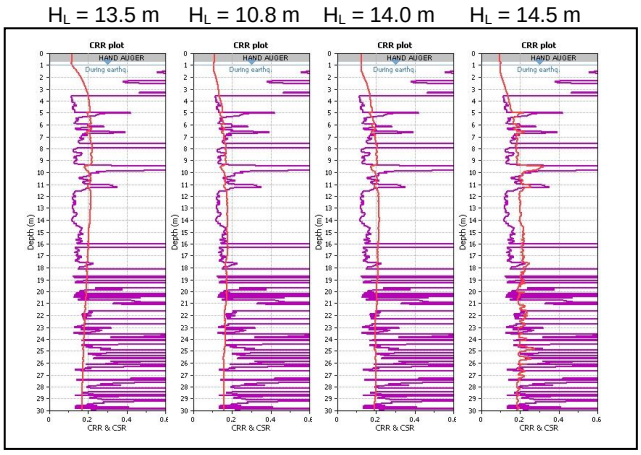


Figure 5 CPT96-01 CSR and CRR versus depth for a) PGA = 0.2g; b) Crustal; c) In-slab; d) Interface

## 7 SOIL LIQUEFACTION MITIGATION

To reduce the consequences of potential soil liquefaction, densification of the underlying soil layers was recommended within the building. The bottom feed, dry method of vibro-replacement was proposed by the specialist contractors as their preferred ground improvement method to densify the soils. Stone columns with 900 mm nominal diameter laid out in a triangular grid pattern at 3 m axis-to-axis horizontal spacing were considered adequate by the specialist contractor. Due to economic and site constraints with this project, the vibro-replacement was carried out to a depth of 14 m below the top of floor slab design elevation and extended to the perimeter of the building.

For quality control purposes during soil densification, five additional CPTs were carried out before starting the mitigation and six CPTs were carried out after mitigation. The quality control test holes were grouped in five clusters: four at the corners of the building and one near its centre.

Generally, the results of the CPTs carried out after soil densification showed that the corrected cone tip resistance ($q_t$) exceeded the target values for clean sand strata, where the friction ratio $R_f$ was less than 0.7% and the $I_c$ parameter was less than 2.6.

However, in silty sand or sandy silt zones where $R_f$ was higher than 0.7% and the $I_c$ parameter was higher than 2.6, $q_t$ values after soil densification whereas less than the target value and, generally, equal to the value before soil densification. This shortcoming was attributed to the inherent limitation of the vibro-replacement soil densification method selected by the specialist contractor.

## 8 POST-SEISMIC SETTLEMENT

It is generally acknowledged that three factors can contribute to post-seismic settlement of buildings:

a) Volumetric ground deformations resulting from localized partial drainage and post-liquefaction reconsolidation, also known as free-field vertical and horizontal deformations;
b) Shear ground deformations induced by soil-structure interaction ratcheting and movements due to bearing

pressure of foundations, also known as shear-induced deformations; and,

c) Removal of materials beneath the foundations due to the formation of ejected sediments, also known as ejecta or sand boils.

### 8.1 Post-seismic free-field settlement

The free-field post-seismic settlement were calculated during the soil liquefaction assessment using the empirical integrated CPT-based empirical approach proposed by Zhang, Robertson & Brachman (2002). The commercial software program CLiq was also used for this calculation.

Before soil densification, the calculated free-field post-seismic settlement was estimated to range from 190 mm to 370 mm with a median of 290 mm.

After soil densification, the calculated free-field post-seismic settlement was estimated to range from 135 mm to 245 mm with a median of 200 mm.

### 8.2 Post-seismic free-field horizontal ground deformation

The free-field post-seismic horizontal ground deformation was calculated during the soil liquefaction assessment using the CPT-based empirical integrated approach proposed by Zhang, Robertson & Brachman (2004). A gentle slope of 0.1 % was assumed within the site. The commercial software program CLiq was also used for this calculation.

Before soil densification, the calculated horizontal ground deformation was estimated to range from 90 mm to 395 mm with a median of 280 mm.

After soil densification, the calculated horizontal ground deformation was estimated to range from 90 mm to 211 mm with a median of 168 mm.

### 8.3 Post-seismic building settlement

The estimation of liquefaction induced building settlement was carried out using the simplified procedure proposed by Bray and Macedo (2017). The commercial software program CLiq was used for this calculation.

This procedure is based on the regression analysis of many cases of nonlinear dynamic soil-structure interactions (SSI) effective stress analyses. These SSI analyses were calibrated and validated by centrifuge tests.

The parameters required for this calculation include: building width (B) in meters, foundation embedment depth ($D_f$) in meters, foundation bearing pressure (Q) in kPa, earthquake spectral acceleration at one second period ($S_{a1}$) in g, the standardized version of the cumulative absolute velocity ($CAV_{dp}$) in g-s defined in Campbell and Bozornia (2011), the total thickness of liquefiable soil ($H_L$) in meters, and the liquefaction-induced building settlement index (LBS), which can be derived from Zhang et al (2004)..

The performance of the proposed methodology was also tested for several well-documented field case histories after the Kocaeli earthquake (August 17, 1999 $M_w$=7.5) and the 2010-2011 Canterbury earthquake sequence, which included the Christchurch event on February 22, 2011 ($M_w$=6.2), the Darfield event on September 4, 2010 ($M_w$=7.1), and the June event on June 13, 2011 ($M_w$=6.0).

The procedure proposed by Bray and Macedo (2017) involved the following steps:

8.3.1 The safety factor against liquefaction triggering ($FS_{LIQ}$) is calculated using the CPT-based Boulanger and Idriss (2016) procedure. The thickness of the liquefiable soil layer ($H_L$) is estimated as the summation of the layers with $FS_{LIQ}$ values lesser than 1.0. The soil liquefaction assessment in Section 5.0 of this paper summarizes the results of this step.

8.3.2 The post-liquefaction soil bearing capacity safety factor (FS) is calculated using the Meyerhof and Hanna (1978) method. With a post-liquefaction residual strength of the liquefied soil layer of 12 kPa, based on Idriss and Boulanger (2008) and using an average shear strength of the non-liquefied crust layer of 20 kPa, based on CPT96-01, the post-liquefaction soil bearing capacity FS was estimated at less than 1.0 and significant liquefaction-induced building settlement was expected to occur.

8.3.3 The estimated LSN (Van Ballegooy et al. 2015) at the corners of the building before soil densification ranged from 17 to 26 and LPI values (Iwasaki et al. 1982) ranged from 15 to 24. After soil densification, both LSN and LPI estimated values were reduced by half. Considering the relatively low LSN and LPI values at the corners of the building and considering the Ishihara (1985) ground failure design chart, ejecta were expected to be minor.

8.3.4 The one-dimensional post-liquefaction volumetric-induced building settlement ($D_v$) is estimated using the Zhang et al. (2002) procedure.

For the NE corner of the building, $D_v$ was estimated to be 206 mm before densification and 139 mm after densification.

For the NW corner of the building, $D_v$ was estimated to be 229 mm before densification and 161 mm after densification.

For the SE corner of the building, $D_v$ was estimated to be 310 mm before densification and 182 mm after densification.

For the SW corner of the building, $D_v$ was estimated to be 263 mm before densification and 163 mm after densification.

8.3.5 LBS is estimated using the Zhang et al. (2004) procedure with the $FS_{LIQ}$ values for each layer estimated previously. The shear-induced building settlement ($D_s$) due to liquefaction was estimated with the following input parameters: $S_{a1}$=0.50g, $CAV_{dp}$= 2.5 *g-s*, B=37 m, Q=80 kPa.

8.3.6 After soil densification, the median estimate of the total liquefaction-induced building settlement ($D_t$) of the NW corner of the building was:

$D_t = D_e + D_v + D_s$ = 0 mm + 161 mm + 87 mm = 248 mm, with $D_t$ ranging from 214 mm to 304 mm.

The median estimate of the total liquefaction-induced building settlement ($D_t$) of the NE corner of the building was:
$D_t = D_e + D_v + D_s$ = 0 mm + 139 mm + 71 mm = 210 mm, with $D_t$ ranging from 182 mm to 257 mm.
The median estimate of the total liquefaction-induced building settlement ($D_t$) of the NW corner of the building was:
$D_t = D_e + D_v + D_s$ = 0 mm + 161 mm + 87 mm = 248 mm, with $D_t$ ranging from 214 mm to 304 mm.
The median estimate of the total liquefaction-induced building settlement ($D_t$) of the SE corner of the building was:
$D_t = D_e + D_v + D_s$ = 0 mm + 182 mm + 91 mm = 273 mm, with $D_t$ ranging from 237 mm to 332 mm.
The median estimate of the total liquefaction-induced building settlement ($D_t$) of the SW corner of the building was:
$D_t = D_e + D_v + D_s$ = 0 mm + 130 mm + 78 mm = 208 mm, with $D_t$ ranging from 177 mm to 258 mm.

Considering the results of the analyses presented above, the estimated median differential settlement across the northern edge of the building was 248 mm – 210 mm = 38 mm and across the southern edge: 273 mm – 208 mm = 65 mm.
The estimated median differential settlement across the western edge of the building was:
248 mm – 208 mm = 40 mm and across the eastern edge: 273 mm – 210 mm = 65 mm.

Figure 6 and Table 3 show a summary of the estimated post-seismic building settlement before and after soil densification.

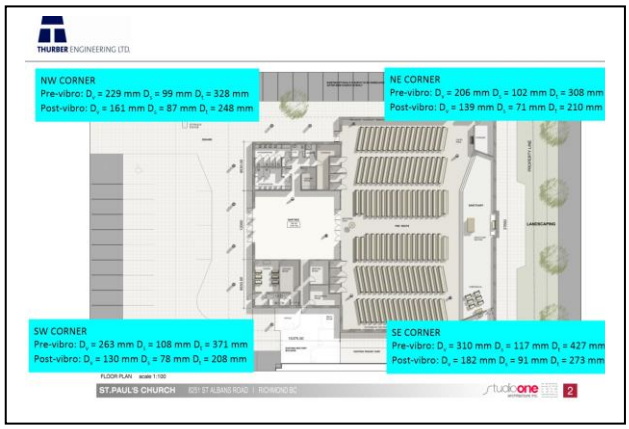


Figure 6 Estimated post-seismic building settlement before and after soil densification

## 9 PRELOADING

Following soil densification by vibro-replacement within the proposed building area, the site preparation also included preloading to El. 4.0 m using compacted Fraser River sand.

Preloading was carried out to reduce, but not eliminate, long-term post-construction settlement of the proposed building. The fill area was setback a minimum of 4 m from the existing adjacent buildings using concrete lock blocks.

The measured settlement after one-month preloading ranged from 10 to 35 mm.

Table 3 Calculated post-seismic building settlement before and after soil densification

| | Estimated building settlement before soil densification | | | |
|---|---|---|---|---|
| Test Hole No. | Pre CPT17-01 | Pre CPT17-04 | Pre CPT17-02 | Pre CPT17-05 |
| Location | NW Corner | NE Corner | SW Corner | SE Corner |
| $D_v$ (mm) | 229 | 206 | 263 | 310 |
| $H_L$ (m) | 10.7 | 9.4 | 11.4 | 13.4 |
| LBS | 22 | 26 | 28 | 33 |
| $D_s$ (mm) | 99 | 102 | 108 | 117 |
| $D_s + \sigma$ (mm) | 163 | 168 | 178 | 193 |
| $D_s - \sigma$ (mm) | 60 | 62 | 65 | 71 |
| $D_v + Ds$, mm | 328 | 308 | 371 | 427 |
| $D_v + (D_s + \sigma)$, mm | 392 | 374 | 441 | 503 |
| $D_v + (D_s - \sigma)$, mm | 289 | 268 | 328 | 381 |

| | Estimated building settlement after soil densification | | | |
|---|---|---|---|---|
| Test Hole No. | Post CPT17-06 | Post CPT17-04 | Post CPT17-03 | Post CPT17-05 |
| Location | NW Corner | NE Corner | SW Corner | SE Corner |
| $D_v$ (mm) | 161 | 139 | 130 | 182 |
| $H_L$ (m) | 8.1 | 6.2 | 8.2 | 8.7 |
| LBS | 16 | 13 | 14 | 19 |
| $D_s$ (mm) | 87 | 71 | 78 | 91 |
| $D_s + \sigma$ (mm) | 143 | 118 | 128 | 150 |
| $D_s - \sigma$ (mm) | 53 | 43 | 47 | 55 |
| $D_v + Ds$, mm | 248 | 210 | 208 | 273 |
| $D_v + (D_s + \sigma)$, mm | 304 | 257 | 258 | 332 |
| $D_v + (D_s - \sigma)$, mm | 214 | 182 | 177 | 237 |

Input parameters: $S_{a1}$ = 0.5g $C_{swp}$ = 2.5 g-s B = 37 m $D_f$ =1.6 m Q = 80 kPa

## 10 SEISMIC DRAINS

After removal of the preload and construction of the building foundations, vertical seismic drains were installed along the building perimeter foundations. The purpose of the seismic drains was to prevent migration of pore water pressure from the non-densified area into the densified area.

The drains were installed down to 9 m depth, with a horizontal spacing of 1.73 m center-to-center, using a sonic drill rig. The drains consisted of corrugated high density polyethene tube (HDPE) of 114 mm outside diameter with a minimum of 4 evenly spaced perforations enclosed in a tight-fitting non-woven filter fabric sock with a maximum apparent opening size (AOS) of 0.21 mm.

The cut-off top of the seismic drains were wrapped with the filter fabric sock and covered with a 28-gauge 3.2-mm stainless wire mesh secured using Thomas & Bett UV black plastic twist cable ties.

The tops of the seismic drains were embedded in the granular fill surrounding the building perimeter.

## 11 CONCLUSIONS

The state-of-the practice still largely involves estimating building settlement using empirical procedures developed to calculate post-liquefaction 1D reconsolidation settlement in the free-field away from buildings. These free-field analyses cannot possibly capture shear-induced deformations in the soil beneath shallow foundations.

The simplified procedure proposed by Bray and Macedo (2017) provides a rational approach for estimating liquefaction-induced building settlement. However, the proposed procedure is a simplification of an inherently complex phenomenon. The proposed procedure was applicable to this project since the building had a regular simple configuration and the subsurface conditions were not highly variable.

The estimated total liquefaction-induced building settlement after soil densification, which included the one-dimensional post-liquefaction volumetric-induced building settlement and the shear-induced building settlement were considered acceptable. The estimated average differential settlement across the building was also considered tolerable by the building structure.

ACKNOWLEDGEMENTS

The writers would like to acknowledge the comments by several anonymous reviewers.

REFERENCES

Anderson, D.L., Byrne, P.M., DeVall, R.H., Naesgaard, E., and Wijewickreme, D., Editors & Contributing Authors. 2007. Task Force Report on Geotechnical design guidelines for buildings on liquefiable sites in Greater Vancouver in accordance with NBC2005," University of British Columbia publication.

Boulanger, R.W. and Idriss I.E. 2014. CPT and SPT based liquefaction triggering procedures. Report Number UCD/CGM-14/01. Department of Civil and Environmental Engineering, University of California at Davis.

Bray, J.D. and Macedo, J. 2017. Simplified procedure for estimating liquefaction-induced building settlement. Proceedings of the 19th International Conference on Soil Mechanics and Geotechnical Engineering. Seoul.

Bray, J.D. and Macedo, J. 2017. 6th Ishihara lecture: Simplified procedure for estimating liquefaction-induced building settlement. Soil Dynamics and Earthquake Engineering.102: 215-231.

Campbell, K. W., and Bozorgnia, Y. 2011. Prediction equations for the standardized version of cumulative absolute velocity as adapted for use in the shutdown of U.S. nuclear power plants. Soil Dynamics and Earthquake Engineering. 241: 2558–2569.

Hunter, J. A., Christian, H.A., Harris, A.J. B., Britton, J.R. and Luternauer, J.L. 1999. Mapping Shear Velocity Structure beneath the Fraser River Delta Sediments – Preliminary Results. Proceedings of the 8th Canadian Conference on Earthquake Engineering. 101-106.

Hunter, J.A., Benjumea, B., Harris, J.B., Miller, R.D., Pullan, S.E., Burns, R.A. and Good, R.L. 2002. Surface and Downhole Shear Wave Seismic Methods for Thick Soil Site Investigation. Soil Dynamics and Earthquake Engineering. 22: 931-941.

Ishihara, K. and Yoshimine, M. 1992. Evaluation of settlements in sand deposits following liquefaction during earthquakes. Journal of Soils and Foundations. 32(1):173–188.

Iwasaki, T., Arakawa, T., and Tokida, K. (1982). "Simplified procedures for assessing soil liquefaction during earthquakes." Proceedings of the Conference on Soil Dynamics and Earthquake Engineering, Southampton, UK, 925−939.

Liam Finn, W.D., Dowling J., Ventura, C.E. 2016. Evaluating liquefaction potential and lateral spreading in a probabilistic ground motion environment. Soil Dynamics and Earthquake Engineering. 91: 202-208.

McGee, T.M., Hunter, J.A., Spence, R.A. and Luternauer J.L. 1998. Mapping the Shallowest Surface of More Compact Sediments Predating Fraser River Deltaic Deposits. Geological Survey of Canada, Open File 3563.

Meyerhof, G. G., and Hanna, A. M. 1978. Ultimate bearing capacity of foundations on layered soil under inclined load. Canadian Geotechnical Journal, 15 (8): 565-572.

Seed, H.B. and Idriss, I.M. 1970. Soil moduli and damping factors for dynamic response analysis. Report No. EERC 70-10, University of California, Berkeley, CA.

Task Force Report. 2007. Geotechnical design guidelines for buildings on liquefiable sites in accordance with NBC 2005 for Greater Vancouver Region.

Van Ballegooy, S., Lacrosse, V., Simpson, J., and Malan, P. 2015. Comparison of CPT-based simplified liquefaction assessment methodologies based on Canterbury Geotechnical Dataset. Proceedings of the 12th Australia New Zealand Conference on Geomechanics: 618-625. Wellington, New Zealand: NZGS & AGS.

Vucetic, M. and Dobry, R. 1991. Effect of Soil Plasticity on Cyclic Response. ASCE Journal of Geotechnical and Geoenvironmental Engineering, 117: 89-107.

Zhang, G., Robertson, P.K. and Brachman, R.W.I. 2002. Estimating liquefaction-induced ground settlements from CPT for level ground, Canadian Geotechnical Journal, 39: 1168-1180.

Zhang, G., Robertson, P.K. and Brachman, R.W.I. 2004. Estimating liquefaction-induced lateral deformations from SPT and CPT, ASCE, Journal of Geotechnical and Environmental, 130 (8): 861-871.